

Thermal Relic Abundances of Particles with Velocity-Dependent Interactions

James B. Dent,^{1,*} Sourish Dutta,^{2,†} and Robert J. Scherrer^{2,‡}

¹*Department of Physics and School of Earth and Space Exploration,
Arizona State University, Tempe, AZ 85287-1404*

²*Department of Physics and Astronomy, Vanderbilt University, Nashville, TN 37235*

We reexamine the evolution of thermal relic particle abundances for the case where the interaction rate depends on the particle velocities. For the case of Sommerfeld enhancement, we show that the standard analytic approximation, modified in a straightforward way, provides an estimate of the relic particle abundance that is accurate to within 10% (in comparison to < 1 % error for the non-Sommerfeld-enhanced case). We examine the effect of kinetic decoupling on relic particle abundances when the interaction rate depends on the velocity. For the case of pure *p*-wave annihilation, the effect of kinetic decoupling is an increase in the relic abundance, but the effect is negligible when the kinetic decoupling temperature is much less than the chemical decoupling temperature. For the case of Sommerfeld-enhanced *s*-wave annihilations, after kinetic decoupling occurs, annihilations continue to change the particle abundance down to arbitrarily low temperatures, until either matter domination begins or the Sommerfeld effect cuts off. We derive analytic approximations to give the final relic particle abundances for both of these cases.

PACS numbers: 98.80.Cq

I. INTRODUCTION

The calculation of the thermal evolution of particle abundances in the early universe represents one of the earliest and most fundamental applications of particle physics to cosmology [1, 2, 3, 4, 5, 6, 7, 8, 9, 10, 11, 12]. The most important application of this calculation is the determination of the relic dark matter abundance. For the simplest case, that of *s*-wave annihilation, one finds that the final abundance is essentially independent of the mass, and the observed dark matter abundance can be achieved with an annihilation rate of [13] approximately $\langle\sigma v\rangle \sim 3 \times 10^{-26} \text{ cm}^3 \text{ sec}^{-1}$, where $\langle\sigma v\rangle$ is the thermally averaged product of the cross section and relative velocity of the annihilating dark matter particles. This result is quite interesting, as it suggests that physics at the electroweak scale may be responsible for the dark matter.

Recently an interesting twist has emerged in this calculation. Motivated by a desire to explain various anomalous astrophysical backgrounds, a number of investigators have examined the possibility that dark matter annihilation involves a Sommerfeld enhancement, which provides an additional factor of $1/v$ in the dark matter annihilation cross section [14, 15]. The effect of this Sommerfeld enhancement on the thermal relic abundances has been discussed for specific models in [16, 17, 18, 19], and treated more generally by Kamionkowski and Profumo [14] and Arkani-Hamed et al. [15]. Note that the latter two papers reached opposite conclusions regarding the effect of Sommerfeld-enhanced annihilations on the relic abundance. Kamionkowski and Profumo estimated a sig-

nificant suppression, while Arkani-Hamed et al. argued for a very small effect. However, these two conclusions are not actually inconsistent, because they rely on different assumptions regarding the strength of the coupling that induces the Sommerfeld enhancement. We will examine both limiting cases in our discussion below.

In this paper, we consider several new aspects of velocity dependent interactions, including both Sommerfeld-enhanced *s*-wave annihilations, and pure *p*-wave annihilations. In the next section, we first consider the analytic approximation of [9, 10], modified for the case of Sommerfeld-enhanced *s*-wave annihilations, and show that it provides a good approximation to the relic abundances in this case. We then consider the effects of kinetic decoupling, which increases the rate at which the relic particle temperature declines, and thereby modifies the abundance when the annihilation rate has a velocity dependence. We provide estimates of this effect for both pure *p*-wave annihilation and Sommerfeld-enhanced *s*-wave annihilation. The latter is a significantly larger effect; we find that in this case, annihilations continue to decrease the relic abundance down to arbitrarily late times, until the abundance freezes out either at the onset of matter domination, or when the Sommerfeld effect itself cuts off. Although calculations of this sort can always be done numerically for any particular model of a relic particle, it is useful to derive such analytic estimates, since they can be applied to arbitrary models, and can provide qualitative insight into the behavior of such models. While interest in the Sommerfeld enhancement has been spurred by recent astrophysical observations, our discussion here is intended to be as general as possible. Our results are discussed in Sec. III.

*Electronic address: jbdent@asu.edu

†Electronic address: sourish.d@gmail.com

‡Electronic address: robert.scherrer@vanderbilt.edu

II. CALCULATION OF RELIC ABUNDANCES

A. Sommerfeld-enhanced *s*-wave annihilation

Recall first the standard formalism for thermal particle abundances in the early universe [9, 10, 11]. Let n be the number density of a relic particle χ , and n_{eq} be its thermal equilibrium number density. Then

$$\frac{dn}{dt} + 3Hn = -\langle\sigma v\rangle(n^2 - n_{eq}^2), \quad (1)$$

where H is the Hubble parameter. To eliminate the expansion term, we express the number density in terms of $Y \equiv n/s$, where s is the total entropy of the universe, and we change the independent variable to $x = m/T$. Further, following [9, 10], we parametrize the cross-section as

$$\langle\sigma v\rangle = \sigma_0 x^{-n}, \quad (2)$$

where $n = 0$ corresponds to *s*-wave annihilation, $n = 1$ for *p*-wave annihilation, and so on. Note that [11] provides a more sophisticated treatment of $\langle\sigma v\rangle$, but at the level of accuracy we are interested in here, equation (2) will be sufficient. For all of the specific cases examined here, we take $\sigma_0 = 3 \times 10^{-26} \text{ cm}^3 \text{ s}^{-1}$. Then equation (1) becomes [9, 10]

$$\frac{dY}{dx} = -\lambda x^{-n-2}(Y^2 - Y_{eq}^2), \quad (3)$$

where the constant λ is given by

$$\lambda = \sqrt{\pi/45}(g_{*S}/g_*^{1/2})m_{Pl}m_\chi\sigma_0, \quad (4)$$

with $m_{Pl} = 1/\sqrt{G}$. Here g_* is the effective number of relativistic degrees of freedom in the universe, defined by the requirement that the energy density in relativistic particles is $\rho_R = (\pi^2/30)g_*T^4$, while g_{*S} is defined in terms of the entropy density s as $s = (2\pi^2/45)g_*T^3$. For the cases we examine here, it is accurate to take $g_{*S} \approx g_*$, and g_* is given by

$$g_* = 106.75 \quad T > 175 \text{ GeV} \quad (5)$$

$$g_* = 96.25 \quad 175 \text{ GeV} > T > 80 \text{ GeV} \quad (6)$$

$$g_* = 86.25 \quad 80 \text{ GeV} > T > 4 \text{ GeV} \quad (7)$$

$$g_* = 75.75 \quad 4 \text{ GeV} > T > 150 \text{ MeV} \quad (8)$$

$$g_* = 17.25 \quad 150 \text{ MeV} > T > 20 \text{ MeV} \quad (9)$$

$$g_* = 10.75 \quad T < 20 \text{ MeV} \quad (10)$$

For the case of interest here, the relic particles can be assumed to be nonrelativistic, so that Y_{eq} is well-approximated by Maxwell-Boltzmann statistics:

$$Y_{EQ} = .145(g_\chi/g_*)x^{3/2}e^{-x} \equiv ax^{3/2}e^{-x}, \quad (11)$$

where g_χ is the number of degrees of freedom of the χ particle.

At early times, the relic particle is in thermal equilibrium, so that its abundance tracks the equilibrium abundance, but at late times the abundance freezes out to a constant value. This argument can be made more explicit by defining the quantity $\Delta \equiv Y - Y_{eq}$, the evolution of which is given by

$$\frac{d\Delta}{dx} = -\frac{dY_{eq}}{dx} - \lambda x^{-n-2}\Delta(2Y_{eq} + \Delta). \quad (12)$$

The approximation in [9] and [10] amounts to setting the right-hand side of equation (12) to zero up to x_f , the value of x at which the abundance freezes out, and then integrating equation (12) for $x > x_f$ with the assumption that both Y_{eq} and dY_{eq}/dx are negligible. One then obtains [9, 10]

$$x_f = \ln[(n+1)a\lambda] - (n+1/2)\ln[\ln[(n+1)a\lambda]], \quad (13)$$

and the final value of Y is

$$Y_\infty = \frac{3.79(n+1)x_f^{n+1}}{(g_{*S}/g_*^{1/2})m_{Pl}m_\chi\sigma_0}. \quad (14)$$

This approximation agrees with the exact integration of the Boltzmann equation to within a few percent. For the case of *s*-wave annihilations, the evolution of Δ is compared to the approximate evolution in Fig. 1 for a 500 GeV particle.

Now consider what happens for *s*-wave annihilations that are Sommerfeld enhanced. Sommerfeld enhancement arises from a long-range attractive force due to a light force carrier ϕ . In the limit where $m_\phi \rightarrow 0$, the annihilation cross-section is enhanced by the factor [15]

$$S = \frac{\pi\alpha/v}{1 - e^{-\pi\alpha/v}}, \quad (15)$$

where v is the velocity of the annihilating particles, and $4\pi\alpha$ is the square of the coupling.

Clearly, the magnitude of the Sommerfeld enhancement depends on the value of α . We illustrate this effect in Fig. 1, showing how the evolution of the particle abundance depends on α . Clearly, for $\alpha \lesssim 0.01$, the effect of the Sommerfeld enhancement on the final relic particle abundance is negligible. On the other hand, for $\pi\alpha/v \gg 1$, equation (15) reduces to a $1/v$ enhancement in the annihilation cross-section. Fig. 1 shows that this limit is achieved for $\alpha \gtrsim 0.3$. Note that [14] and [15] assumed these opposite limiting behaviors in deriving their estimates of the effect on the thermal relic abundance. The case $0.01 \gtrsim \alpha \gtrsim 0.3$, gives an intermediate regime displayed in Fig. 1. Since $1/v$ enhancement provides one set of limiting behaviors, we will assume a simple $1/v$ enhancement in what follows.

Note that the effect is more complex if one does not assume $m_\phi \rightarrow 0$; in this case, the production of bound states results in resonant enhancement of the annihilation rate, while at the same time the Sommerfeld enhancement cuts off for $v < m_\phi/m_\chi$ [15]. We will consider only

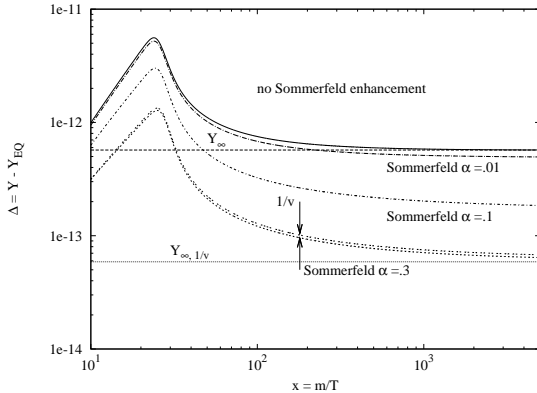


FIG. 1: The evolution of relic particle densities for the case of Sommerfeld-enhanced s -wave annihilations of a 500 GeV mass particle with $\sigma_0 = 3 \times 10^{-26} \text{ cm}^3 \text{ s}^{-1}$ as a function of the indicated value of the coupling α . Top and bottom curves correspond to the limiting cases of no Sommerfeld enhancement, and $1/v$ enhancement. Horizontal lines are the analytic estimates for the final relic abundances in these two cases (i.e. $n = 0$ and $n = -1/2$, respectively, in equations 13 and 14).

the case $m_\phi \rightarrow 0$, but will discuss these other effects qualitatively later.

A nonrelativistic particle has a velocity that scales as $\langle v^2 \rangle \propto T_\chi$. As long as the particle is in thermal equilibrium, $T_\chi = T$. Hence the effect of Sommerfeld annihilation is to modify equation (3) (for $n = 0$) to the form

$$\frac{dY}{dx} = -\lambda x^{-3/2} (Y^2 - Y_{eq}^2). \quad (16)$$

It would appear, then, that the relic abundance in this case is well-approximated by the standard freeze-out abundance for the case $n = -1/2$ in Eqs. (13) and (14). Indeed, this was the assumption made in Ref. [14]. However, it is not *a priori* obvious that equations (13) and (14) can be accurately applied in the regime $n < 0$, since they have been numerically tested only in the regime $n > 0$, and the freeze-out process becomes progressively less “sharp” as n decreases. In Fig. 1, we integrate the Boltzmann equation for the same set of parameters, but with a $1/v$ enhancement in the annihilation rate. The final abundance is reasonably well-approximated by the $n = -1/2$ analytic approximation, but the agreement with the exact numerical results is not quite as good as for the s -wave case without the Sommerfeld effect.

This result allows us to estimate the ratio between the abundance in the presence of Sommerfeld enhancement, Y_∞^{SOM} to the standard s -wave abundance without Sommerfeld enhancement, Y_∞ . We obtain

$$\begin{aligned} \frac{Y_\infty^{SOM}}{Y_\infty} &= \frac{1}{2} \frac{x_{fSOM}^{1/2}}{x_f}, \\ &= \frac{1}{2} \frac{\sqrt{\ln(a\lambda/2)}}{\ln(a\lambda) - (1/2)\ln\ln(a\lambda)}. \end{aligned} \quad (17)$$

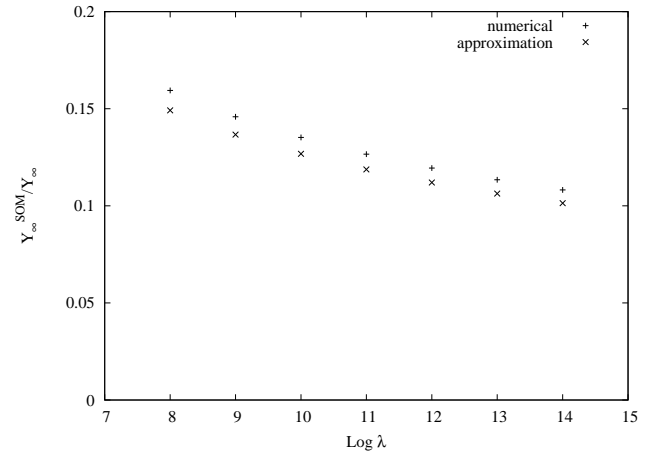


FIG. 2: A comparison between the analytic approximation for the ratio in relic abundance for s -wave annihilation with and without a $1/v$ Sommerfeld enhancement to the corresponding numerical results over several orders of magnitude of the parameter λ .

Here x_{fSOM} is the value of x_f when Sommerfeld enhancement is included. Taking $x_{fSOM} \approx x_{f0}$ yields the abundance estimate given in [14]. Our results confirm that the change in the x_f is indeed very small. For the standard dark matter freeze-out value of $x_f = 20$, we find that x_{fSOM} is larger by only a few percent, while equation (17) gives $Y_\infty^{SOM}/Y_\infty \sim 1/10$. Both of these results are confirmed numerically in Fig. 1. In Fig. 2, we compare the estimate given by equation (17) to numerical results. The analytic estimate differs from the numerical result by about 10%. In contrast, the analytic abundance estimate for s -wave annihilation without Sommerfeld enhancement is accurate to within 1% [9].

B. Effects of Kinetic Decoupling

The results in the previous section assume that the temperature of the relic annihilating particle tracks the background radiation temperature. This will be true as long as the annihilating particle remains in thermal equilibrium with the radiation background. However, once the particle drops out of thermal equilibrium, we expect its temperature to scale as $T_\chi \propto 1/R^2$, where R is the scale factor, while the radiation temperature scales as $T \propto 1/R$.

Thus, we need to make the standard distinction between chemical equilibrium and kinetic equilibrium. The freeze-out process we have discussed above is actually the process by which the annihilating relic particle drops out of chemical equilibrium, so that number-changing interactions are no longer effective, and the particle’s comoving number density becomes constant. However, even after dropping out of chemical equilibrium, the relic particle will, in general remain in kinetic equilibrium as it continues to scatter off of relativistic standard model par-

ticles which are in local thermal equilibrium with the radiation background. As long as the particle is in kinetic equilibrium, its temperature tracks the background radiation temperature. Finally, at some kinetic decoupling temperature, T_k , the scattering interactions are no longer sufficient to maintain kinetic equilibrium, and the temperature of the particle decreases as $1/R^2$ rather than $1/R$. (For a recent discussion, see, e.g., [20, 21, 22, 23]).

The precise temperature at which kinetic decoupling occurs is dependent on the model for the relic particle of interest. For instance, in the set of supersymmetric models examined in [23], $T_k/T_f \sim 10^{-1} - 10^{-3}$. Since we wish to keep our discussion as general as possible, we will take T_k/T_f as a free parameter, subject only to the constraint that $T_k \leq T_f$, since number-changing interactions also maintain kinetic equilibrium. We also make the approximation that the particle drops out of kinetic equilibrium instantaneously at T_k ; this is a reasonable approximation [22, 23]. With these assumptions, the relation between T_χ and T is

$$T_\chi = T^2/T_k. \quad (18)$$

The change in the evolution of T_χ brought about by kinetic decoupling changes the velocity evolution of the annihilating particles, since $v \propto T_\chi^{1/2}$ for nonrelativistic particles. Since the standard s -wave annihilation cross section, $\langle \sigma v \rangle$, is independent of T_χ (or equivalently, v_χ), kinetic decoupling has no effect in this case. The same is not true for p -wave annihilation, for which $\langle \sigma v \rangle \propto T_\chi$, or for Sommerfeld-enhanced s -wave annihilation, for which $\langle \sigma v \rangle \propto T_\chi^{-1/2}$. The reverse reactions (which create χ) can be neglected during the era following kinetic decoupling, since $T_k \leq T_f$. Thus, the Boltzmann equation following kinetic decoupling for p -wave annihilation becomes

$$\frac{dY}{dx} = -\lambda x_k x^{-4} Y^2, \quad (19)$$

where we define the constant $x_k = m/T_k$. For Sommerfeld-enhanced s -wave annihilation, we obtain:

$$\frac{dY}{dx} = -\lambda x_k^{-1/2} x^{-1} Y^2. \quad (20)$$

The effect of kinetic decoupling on the final relic abundances is easy to estimate. Recall that equation (14) is derived by integrating the annihilation portion of the Boltzmann equation (only) from $x = x_f$ to ∞ [9, 10]. Replacing this integration by an integration from x_f to x_k , and then integrating equations (19) and (20) from x_k to ∞ should provide the correct estimate of the change in the final relic abundance.

For p -wave annihilation, we obtain the ratio between the final abundance in the presence of kinetic decoupling, $Y_\infty^{(k)}$, and the abundance in the limit where the particle stays in kinetic equilibrium to an arbitrarily low temperature, Y_∞ . This ratio is

$$\frac{Y_\infty^{(k)}}{Y_\infty} = \frac{1}{1 - (1/3)(T_k/T_f)^2}. \quad (21)$$

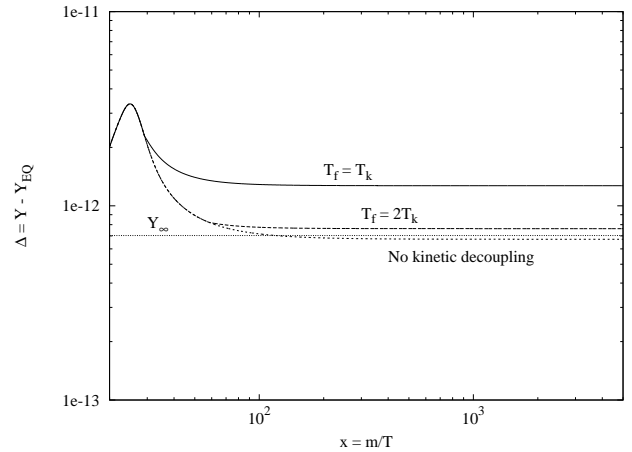


FIG. 3: The effect of kinetic decoupling on the evolution of the relic particle abundance for the case of p -wave annihilation of a 500 GeV mass particle with $\sigma_0 = 3 \times 10^{-26} \text{ cm}^3 \text{ s}^{-1}$. Horizontal line gives our analytic estimate of the final relic abundance.

We see that the effect of kinetic decoupling is to increase the final relic abundance for the case of p -wave annihilations. This is easy to understand, since the annihilation rate in this case scales as T_χ , so a more rapid decrease in T_χ due to kinetic decoupling leads to fewer relic annihilations after freeze-out, and so a larger relic abundance. The effect, however, rapidly becomes irrelevant for $T_k/T_f \ll 1$. For example, for $T_k/T_f = 1/2$, the result is a 9% increase in the relic abundance. For $T_k/T_f < 0.1$, the increase in the relic abundance is less than 0.3%. A numerical calculation of this effect is illustrated in Fig. 3. Since the effect of kinetic decoupling becomes significant only for values of T_k/T_f that are implausibly large, it is unlikely to be of much importance for p -wave annihilation.

The effect of kinetic decoupling is much more striking for the case of Sommerfeld-enhanced s -wave annihilations. In this case, an integration of equation (20) shows that annihilations never terminate: after kinetic decoupling, $Y \sim 1/\ln x$. (This case has previously been discussed briefly in [9, 15]). However, this process will eventually be cut off by one of two possibilities. First, as noted earlier, Sommerfeld enhancement saturates once the velocity drops to $v \sim m_\phi/m_\chi$, at which point normal s -wave annihilations resume. Second, our calculation holds only for the radiation-dominated case, and freeze-out will occur rapidly once matter domination begins. Let T_{cutoff} be the radiation temperature at which the Sommerfeld effect cuts off or matter domination begins, whichever is larger. Then we can again integrate the equations governing particle annihilation from x_f to x_k with $T_\chi = T$, and from x_k to x_{cutoff} with $T_\chi = T^2/T_k$, where freeze-out then occurs with negligible further an-

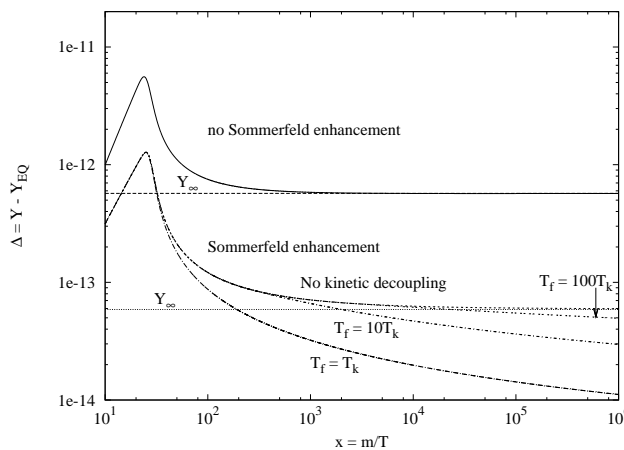


FIG. 4: The effect of kinetic decoupling on the evolution of the relic particle abundance for the case of *s*-wave annihilation for a 500 GeV mass particle with $\sigma_0 = 3 \times 10^{-26} \text{ cm}^3 \text{ s}^{-1}$, in the limit where the Sommerfeld enhancement scales as $1/v$. Horizontal lines give our analytic estimates of the final relic abundances.

nihilations at T_{cutoff} . We find

$$\frac{Y_\infty^{(k)}}{Y_\infty} = (T_f/T_k)^{1/2} \left(\sqrt{\frac{T_f}{T_k}} - 1 + \frac{1}{2} \ln(T_k/T_{cutoff}) \right)^{-1}. \quad (22)$$

The effect of kinetic decoupling with Sommerfeld-enhanced annihilations is illustrated numerically in Figs. 4 and 5. In Fig. 4, we show the evolution of the particle abundance for the case we have just considered ($1/v$ enhancement), while Fig. 5 shows the case $\alpha = 0.01$ (of course, our analytic estimate, equation (22), does not apply in the latter case.) Fig. 5 illustrates the fact that a value of the coupling for Sommerfeld enhancement can be small enough to produce a negligible change in the relic abundance without kinetic decoupling, but it can have a large effect once kinetic decoupling occurs.

III. DISCUSSION

We have confirmed that the standard analytic approximation for the relic particle abundances can be applied, with the appropriate modification, to the case of *s*-wave relic abundances in the presence of a Sommerfeld enhanced interaction, although the error in applying this approximation to the case of Sommerfeld-enhanced s-

wave annihilations ($\sim 10\%$) is significantly larger than in the *s*-wave case without Sommerfeld enhancement ($< 1\%$). We have also determined the range of the coupling α over which Sommerfeld annihilation can be either neglected in the calculation of relic densities (as suggested in [15]) or treated purely as a $1/v$ enhancement to the annihilation rate (as in [14]).

When kinetic decoupling occurs, it affects the relic abundances for both *p*-wave annihilations and

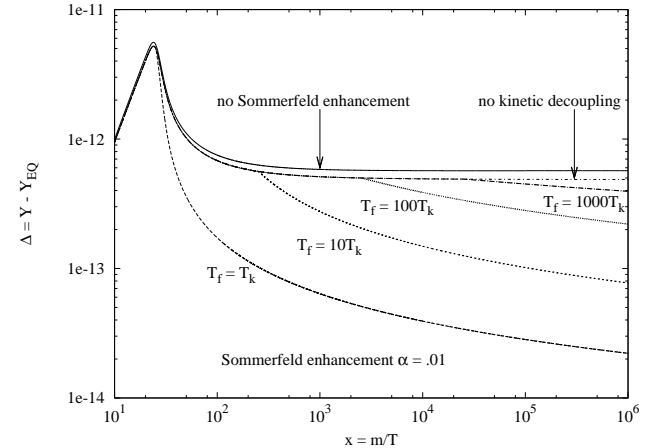


FIG. 5: As Fig. 4, for Sommerfeld-enhancement coupling of $\alpha = 0.01$, a value for which the Sommerfeld effect by itself is negligible without kinetic decoupling. Note the strong effect of kinetic decoupling upon the relic particle abundances.

Sommerfeld-enhanced *s*-wave annihilations. In the former case, the effect is generally very small unless kinetic decoupling occurs at nearly the same epoch as chemical decoupling. For Sommerfeld-enhanced *s*-wave decoupling, the effect is quite large, and we have provided an analytic estimate of this effect.

Acknowledgments

J.B.D., S.D. and R.J.S. were supported in part by the Department of Energy (DE-FG05-85ER40226) at Vanderbilt. J.B.D. also acknowledges support from a Department of Energy grant at Arizona State University and from the Arizona State Foundation. We thank M. Kamionkowski, T.W. Kephart, and L.M. Krauss for helpful discussions.

-
- [1] Ya. B. Zel'dovich, *Adv. Astron. Astrophys.* **3**, 241 (1965).
[2] H.-Y. Chiu, *Phys. Rev. Lett.* **17**, 712 (1966).
[3] B.W. Lee and S. Weinberg, *Phys. Rev. Lett.* **39**, 169 (1977).
[4] P. Hut, *Phys. Lett. B* **69**, 85 (1977).
[5] S. Wolfram, *Phys. Lett. B* **82**, 65 (1979).
[6] G. Steigman, *Ann. Rev. Nucl. Part. Sci.* **29**, 313 (1979).
[7] K. Olive and M.S. Turner, *Phys. Rev. D* **25**, 213 (1982).
[8] L.M. Krauss, *Phys. Lett. B* **128**, 37 (1983).
[9] R.J. Scherrer and M.S. Turner, *Phys. Rev. D* **33**, 1585

- (1986).
- [10] E.W. Kolb and M.S. Turner, *The Early Universe*, (New York: Addison-Wesley, 1990).
 - [11] P. Gondolo and G. Gelmini, Nucl. Phys. B **360**, 145 (1991).
 - [12] K. Griest and D. Seckel, Phys. Rev. D **43**, 3191 (1991).
 - [13] G. Jungman, M. Kamionkowski, and K. Griest, Phys. Rep. **267**, 195 (1996).
 - [14] M. Kamionkowski and S. Profumo, Phys. Rev. Lett. **101**, 261301 (2008).
 - [15] N. Arkani-Hamed, D.P. Finkbeiner, T.R. Slatyer, and N. Weiner, Phys. Rev. D **79**, 015014 (2009).
 - [16] H. Baer, K. Cheung, and J.F. Gunion, Phys. Rev. D **59**, 075002 (1999).
 - [17] J. Hisano, et al., Phys. Lett. B **646**, 34 (2007).
 - [18] M. Cirelli, A. Strumia, and M. Tamburini, Nucl. Phys. B **787**, 152 (2007).
 - [19] J. March-Russell, S.M. West, D. Cumberbatch, and D. Hooper, JHEP **7**, 058 (2008).
 - [20] X. Chen, M. Kamionkowski, and X. Zhang, Phys. Rev. D **64**, 021302 (2001).
 - [21] S. Hofmann, D.J. Schwarz, and H. Stoecker, Phys. Rev. D **64** 083507 (2001).
 - [22] T. Bringmann and S. Hofmann, JCAP **4**, 016 (2007)
 - [23] T. Bringmann, [arXiv:0903.0189].